HHS Public Access

Author manuscript

Magn Reson Med. Author manuscript; available in PMC 2019 January 01.

Published in final edited form as:

Magn Reson Med. 2018 January ; 79(1): 195–207. doi:10.1002/mrm.26661.

k-t accelerated aortic 4D flow MRI in under 2 minutes: feasibility and impact of resolution, k-space sampling patterns, and respiratory navigator gating on hemodynamic measurements

Emilie Bollache[1], **Alex J Barker**[1], **Ryan Scott Dolan**[1], **James C Carr**[1], **Pim van Ooij**[2], **Rouzbeh Ahmadian**[1], **Alex Powell**[1], **Jeremy D Collins**[1], **Julia Geiger**[1,3], and **Michael Markl**[1,4]

[1]Department of Radiology, Feinberg School of Medicine, Northwestern University, Chicago, USA [2]Department of Radiology, Academic Medical Center, Amsterdam, the Netherlands [3]Department of Diagnostic and Interventional Radiology, University Hospital of Würzburg, Würzburg, Germany [4]Department of Biomedical Engineering, McCormick School of Engineering, Northwestern University, Chicago, USA

Abstract

Purpose—To assess the performance of highly accelerated free breathing aortic 4D flow MRI acquired in under 2 minutes compared to conventional respiratory gated 4D flow.

Methods—Eight k-t accelerated non-gated 4D flow MRI (PEAK GRAPPA, R=5, TRes=67.2ms) using four k_y-k_z Cartesian sampling patterns (linear, center-out, out-center-out, random) and two spatial resolutions (SRes1=3.5×2.3×2.6mm^3, SRes2=4.5×2.3×2.6mm^3) were compared *in vitro* (aortic coarctation flow phantom) and in 10 healthy volunteers, to conventional 4D flow (16mm-navigator acceptance window; R=2; TRes=39.2ms; SRes=3.2×2.3×2.4mm^3). The best k-t accelerated approach was further assessed in 10 patients with aortic disease.

Results—k-t accelerated *in vitro* aortic peak flow (Qmax), net flow (Qnet), and peak velocity (Vmax) were lower than conventional 4D flow indices by ≤4.7%, ≤11%, and ≤22%, respectively. *In viv*o k-t accelerated acquisitions were significantly shorter but showed a trend to lower image quality compared to conventional 4D flow. Hemodynamic indices for linear and out-center-out k-space samplings were in agreement with conventional 4D flow (Qmax≤13%, Qnet≤13%, Vmax≤17%, $p>0.05$).

Conclusion—Aortic 4D flow MRI in under 2 minutes is feasible with moderate underestimation of flow indices. Differences in k-space sampling patterns suggest an opportunity to mitigate image artifacts by an optimal trade-off between scan time, acceleration, and k-space sampling.

Keywords

4D flow MRI; aortic hemodynamics; k-t acceleration; navigator gating; k-space sampling; short scan time

Corresponding author: Michael Markl, PhD, Northwestern University - 737 N Michigan ave Suite 1600 - Chicago, Illinois 60611, USA, Telephone: +1-312-695-1799 / Fax: +1-312-926-5991, mmarkl@northwestern.edu.

Introduction

While time-resolved (CINE) 2D phase-contrast (PC) MRI is already an established clinical tool for the non-invasive evaluation of aortic blood flow (1), three-dimensional CINE PC MRI with three-directional velocity encoding (4D flow MRI) has emerged as a more comprehensive tool for the assessment of aortic hemodynamics (2). It allows for both the visualization of blood flow and the retrospective quantification of velocity and flow rate indices at any location inside a 3D volume.

Due to its multi-dimensional nature (3D + time + 3 velocity encoding directions), scan times for 4D flow MRI can be long, hampering its use in clinical routine and preventing the acquisition during a breath-hold, as is common for 2D CINE PC MRI. In addition, respiration control is needed for cardiothoracic applications to reduce breathing-induced blurring and ghosting artifacts (3), rendering the acquisition time even longer. Even with advanced navigator gating and respiration-driven phase encoding (4), scan time efficiency can be 60–80% compared to an ungated sequence, with a typical duration of 8–12 minutes for an aortic 4D flow exam (depending on heart rate and navigator efficiency, using regular parallel imaging with R=2).

Several studies have shown that the application of advanced acceleration techniques can be used to substantially reduce 4D flow scan times. Recent and ongoing developments in sparse sampling techniques, e.g. compressed sensing (5) or radial acquisition (6), as well as multidimensional parallel imaging, e.g. k-t GRAPPA (7–9), have shown great potential to accelerate data acquisition and shorten overall 4D flow scan time. However, the combination of these techniques with free breathing acquisitions, i.e. maintaining a 100% scan efficiency, and different spatio-temporal resolutions has not been systematically investigated.

It was the aim of this study to assess the feasibility of performing aortic 4D flow MRI in under 2 minutes by combining k-t acceleration, free breathing data acquisition using different k_y-k_z sampling patterns (linear, centric, random) to mitigate breathing artifacts, and adapted spatial/temporal resolutions. Our goal was to assess the impact of 8 different 4D flow acquisition strategies on image quality and quantification of flow indices (regional peak velocity as well as peak flow and net flow volume), both *in vitro* in a patient-specific aortic flow phantom and in a study with healthy volunteers in comparison to conventional 4D flow acquired with navigator gating. Finally, the strategy providing the best performance in this preliminary study was further assessed in 10 patients with aortic disease.

Materials and methods

4D flow MRI pulse sequences and k-space reordering strategies

Conventional 4D flow MRI was performed according to consensus recommendations and was further used as the reference method (2). Prospectively ECG gated 4D flow was acquired with respiration control (navigator gating of the lung-liver interface) (10). Parallel imaging (GRAPPA) along phase encoding direction (y) with a reduction factor R=2 (24 reference lines) was used for imaging acceleration. No parallel imaging was applied for the

slice encoding direction (z). Additional pulse sequence parameters are summarized in Table 1.

Highly accelerated 4D flow MRI was achieved using spatio-temporal (k-t) 'PEAK GRAPPA' undersampling and reconstruction technique - an extension of k-t GRAPPA - as reported previously (9,11). Briefly, PEAK GRAPPA is characterized by a uniform reconstruction kernel geometry composing a smallest cell within a k_y-k_z-t data undersampling pattern. Data sampling and reconstruction with a reduction factor of R=5 were used, which demonstrated optimal performance in a previous study (12). The k-t algorithm was integrated into the scanner's data reconstruction workflow and all undersampled data were acquired and reconstructed directly on the MRI system. To assess the impact of data acquisition during free breathing on image quality, different k_y-k_z sampling patterns were investigated. Four Cartesian k_y-k_z-space filling patterns were implemented as described below and illustrated in Figure 1:

1. k_y-k_z-space filled conventionally in a linear line-by-line fashion;
2. k_y-k_z-space filled from the central (k_y=k_z= 0) to the outer k-space positions ('center-out');
3. most outer k_y-k_z-space positions (i.e. k-space corners) initially filled during the first 10 cardiac cycles, followed by centric encoding, as in scheme #2 ('out-center-out');
4. k_y-k_z-space was filled randomly, using a randomized permutation of k_y-k_z-space positions as defined a priori based on the k_y-k_z acquisition matrix size.

Our objective by testing the 'center-out' k-space filling pattern was to prioritize filling of the k-space center at the beginning of the acquisition over as few respiratory cycles as possible, in order to minimize artifacts due to changes in respiration pattern. The 'out-center-out' pattern was based on a combination of the center-out pattern, with an initial filling of the k-space corners at the beginning of the acquisition to ensure stable physiological conditions and respiration patterns when central k-space data was acquired. Finally, the idea behind the random pattern was to average the effect of any potential confounder, by acquiring both center and corners of the k-space independently of the acquisition or respiratory timing.

Spatial and temporal resolutions of k-t accelerated 4D flow MRI were selected to achieve total scan times <2:30 minutes (spatial resolution SRes1) and <2 minutes (spatial resolution SRes2) as summarized in Table 1.

In vitro 4D flow MRI phantom experiments

To systematically evaluate the impact of spatio-temporal resolution and k-t acceleration on 4D flow-derived flow parameters, a patient-specific *in vitro* aorta model was used to perform flow phantom experiments on a 1.5T MAGNETOM Aera scanner (Siemens Medical Systems, Erlangen, Germany). The phantom geometry was created from 3D contrast-enhanced MR angiography (CE-MRA) of a 41-year-old male patient after repair of an aortic coarctation (13) (Supporting Figure S1). 3D segmentation of the thoracic aorta was performed using CE-MRA and dedicated software (Mimics, Materialise). Standard tube

fittings were mated to the segmentation (Solidworks, Waltham, MA, USA) to integrate the model with a previously described MRI-compatible, pulsatile flow loop (14). An STL file was exported (Blender, Freeware) to 3D print a scale model of the aorta using Acrylonitrile-Butadiene-Styrene (ABS) (Makerbot Replicator 2x, Makerbot Industries, NY, USA).

Pulsatile flow was generated by a pneumatically driven ventricular assist device (VAD, volume: 60 ml) (14,15). The VAD and pump control unit (MEDOS, Germany) are approved for clinical use as an artificial ventricle in patients with heart failure. The VAD, which is made of MRI-compatible thermoplastic polyurethane with polycarbonate connectors, comprises pneumatic drive and blood/fluid compartments, separated by a membrane. Pneumatic pressures are applied on the membrane to mimic systole and diastole, during which the fluid is ejected from or filling into the VAD, respectively, through trileaflet aortic valve-shaped valves. The VAD was directly attached to the ascending aorta of the 3D printed model and placed inside the MRI magnet to mimic the beating left ventricle (Supporting Figure S1). The following settings were supplied to the pump control unit outside the MRI room: heart rate=80 bpm, systolic / diastolic pressures=120 / −20 mmHg, systolic period=25% of the entire cardiac cycle. The pump and the MRI trigger were synchronized using LabVIEW (National Instruments, TX, USA). Gadopentetate dimeglumine (Magnevist, Bayer, Germany) was used to enhance the signal-to-noise ratio of the fluid (de-ionized water).

The conventional 4D flow MRI exam, along with a total of eight additional k-t accelerated 4D flow MRI acquisitions (4 different k_y-k_z sampling patterns: linear, center-out, out-center-out, random; 2 spatial resolutions=3.6×2.3×2.6 mm^3 and 4.5×2.3×2.6 mm^3) were performed (see Table 1 for details) with full coverage of the aorta model.

In vivo 4D flow MRI

Twenty subjects were prospectively recruited between July and December 2016 for an Institutional Review Board-approved study with informed consent obtained for all participants.

In a first study, 10 healthy volunteers (4 women, age: 61±16 [31–77] years, weight: 88±21 [59–127] kg) with no history of cardiovascular disease underwent MRI on a 1.5T MAGNETOM Aera scanner (Siemens Medical Systems, Erlangen, Germany). Non-contrast 4D flow MRI was performed in a sagittal oblique volume which included the entire thoracic aorta. Similar to the *in vitro* phantom experiments, a total of nine 4D flow acquisitions were performed for each subject: conventional 4D flow MRI and eight k-t accelerated free breathing 4D flow MRI scans with different k_y-k_z sampling patterns (linear, center-out, out-center-out, random) and two spatial resolutions. Acquisition parameters are provided in Table 1.

Secondly, the k-t accelerated free breathing 4D flow MRI with the best spatial resolution and the k_y-k_z sampling pattern providing the best performance *in vitro* and in the healthy volunteers was further assessed and compared to the conventional gated sequence in 10 patients (3 women, age: 60±10 [44–74] years, weight: 88±13 [73–117] kg) with various aortic disease, on a 1.5T MAGNETOM Avanto scanner (Siemens Medical Systems).

Acquisition parameters were as follows; k-t accelerated 4D flow: TR=4.1 ms, TE=2.2 ms, acquisition matrix=160×80, FOV=360×270 mm^2, spatial resolution=3.4×2.3×2.8–3.0 mm^3, N_{Seg}=4, temporal resolution=65.6 ms, number of slices=24, PEAK GRAPPA R=5; conventional 4D flow: TR=4.8 ms, TE=2.4 ms, acquisition matrix=160×88, FOV=340×276 mm^2, spatial resolution=3.1×2.1×2.6–3.2 mm^3, N_{Seg}=2, temporal resolution=38.4 ms, number of slices=26±1, GRAPPA R=2. For both sequences, a 15° flip angle was used due to the injection of contrast agent (0.2 mmol/kg Gadavist (double dose), Bayer, Leverkusen, Germany). Encoding velocity ranged from 150 to 250 cm/s depending on the presence of aortic valve stenosis.

All scans were performed using prospective ECG gating. The conventional 4D flow MRI sequence (considered as the reference scan) was acquired according to recommendations (2), which included the use of respiratory navigator gating placed on the lung/liver interface, with a fixed 16 mm-acceptance window size combined with respiratory-ordered phase encoding (10). For each 4D flow MRI sequence, the acquisition time was recorded.

Flow quantification

For each *in vitro* and *in vivo* 4D flow dataset, preprocessing was applied using a previously described tool programmed in Matlab (The Mathworks, USA) (16), including eddy current correction and background noise suppression. A 3D angiogram (PC-MRA) was computed (16) to segment the aortic volume (Mimics, Materialize) and subsequently mask the flow velocities.

Next, sagittal maximal intensity projections (MIP) of the systolic absolute velocities inside the 3D segmentation were calculated and used to obtain the regional peak velocity (Vmax) in the ascending (AA) and proximal descending (DA) aorta, as well as in the aortic arch, while excluding the supra-aortic branches (see Figure 2a) (17). Finally, 2D planes were manually positioned in the AA and DA orthogonal to the aortic axis at the level of the pulmonary artery using commercial software (EnSight, CEI, Apex, North Carolina, USA). Peak flow (Qmax) and net flow (throughout the cardiac cycle, Qnet) were computed after segmenting AA and DA borders (custom software programmed in Matlab) (18).

Image quality assessment

To evaluate the impact of navigator gating, image quality was assessed in each *in vivo* 4D flow dataset in a randomized order by a blinded radiologist with 10 years of experience. Assessment was based on the 4D flow magnitude cine data and the PC-MRA sagittal MIP. Edge sharpness of the aortic wall as well as signal and noise inside the aorta were graded on a 3-point scale (1: low, 2: medium, 3: high quality), separately in the AA, arch and DA.

Statistical analysis

Image quality grading median values along with interquartile ranges separately over the 10 healthy volunteers and 10 patients were reported for each 4D flow acquisition. AA, DA peak velocity (Vmax), flow peak (Qmax) and net volume (Qnet), as well as arch Vmax, averaged over each healthy and disease population, were provided as mean ± standard deviation. Each dataset obtained from non-respiratory controlled k-t accelerated 4D flow sequences was

compared against conventional 4D flow measurements as a reference: Bland-Altman analysis was employed to calculate mean biases and limits of agreement (as defined by mean bias ± 1.96 x standard deviation) for each hemodynamic index (AA and DA Vmax, Qmax and Qnet, as well as arch Vmax). The significance of the differences for each index, as well as scan time and image quality grading, was tested using a Wilcoxon signed rank test. Finally, relative differences as defined as non-gated - gated measurements were reported for each index, in percentage of the gated measurement.

In addition, for each 4D flow acquisition, AA and DA flow rate waveforms were interpolated using a 1 ms-time step and then averaged over the 10 volunteers as well as the 10 patients. Comparison at time points every 38 ms was performed using a Kruskal-Wallis test across the 9 sequences in the volunteers and a Wilcoxon signed rank test between the 2 sequences in patients. A p value <0.05 was considered as statistically significant. Statistical analyses were performed using Matlab (MathWorks, Natick, MA, USA).

Results

For the *in vitro* and all *in vivo* scans, the conventional and k-t accelerated 4D flow MRI datasets were successfully acquired, resulting in a total number of n=119 4D flow MRI datasets (9 *in vitro*, 110 *in vivo*).

In vitro 4D flow MRI phantom experiments

Total scan time was 9:27, 2:16 and 1:53 minutes for the conventional 4D flow MRI and the k-t accelerated acquisitions with spatial resolutions of 3.6×2.3×2.6 mm^3 and 4.5×2.3×2.6 mm^3, respectively.

Aortic velocity MIP as well as AA and DA flow waveforms over the cardiac cycle are shown in Figure 2 for linear k-space reordering and Supporting Figure S2 for all eight k-t accelerated acquisitions, clearly illustrating the ability of the 2-minute 4D flow MRI scans to reproduce peak systolic velocity and flow patterns. Quantitative AA and DA peak velocity (Vmax), flow peak (Qmax) and net volume (Qnet), as well as arch Vmax, are provided for each dataset in Table 2, along with percentage differences when compared to conventional 4D flow measurements. The relative error for Vmax ranged from −13 to −0.8% in the AA and arch, while it reached down to −22% in regions with accelerated and complex flow near the coarctation in the DA. Overall small differences were observed for flow indices: −4 to 4.7% for Qmax, −2.7 to 11% for Qnet, with the most optimal performance for the ‘out-center-out’ k_y-k_z sampling pattern (absolute differences ranging from Vmax: −18 to −0.8%; Qmax: −1.9 to 4.2%; Qnet: −1.9 to 9.8%).

Volunteer study: scan times

Scan times for the conventional respiration-controlled 4D flow MRI as well as for free breathing k-t accelerated 4D flow MRI are provided in Table 3. They were significantly reduced for all eight k-t accelerated 4D flow MRI sequences by 7:52–12:19 minutes when compared to conventional 4D flow (p=0.002). Of note, conventional 4D flow scan time included 1:05±0:21 minutes to set up navigator crossed-pair slices at the diaphragm level, and average scan efficiency was 74±14 [50–100]%. For each volunteer and each k_y-k_z

sampling pattern, scan time was below 2 minutes for acquisitions with the spatial resolution SRes2.

Volunteer study: image quality

Figure 3 illustrates examples of 4D flow magnitude images and 3D PC-MRA MIP in sagittal orientation for conventional 4D flow as well as k-t accelerated 4D flow data using linear k-space filling and two different spatial resolutions. Image quality grading obtained with each k-t accelerated dataset for edge sharpness, signal and noise in the AA, arch and DA, along with comparison against conventional 4D flow MRI are provided in Table 4. Overall a trend towards reduced image quality was found for k-t accelerated 4D flow data when compared against conventional 4D flow. However, most image quality differences were not significantly different for aortic wall edge sharpness, signal or noise except for a number of aortic segments for linear, out-center-out and random k-space ordering strategies for SRes1.

Volunteer study: flow quantification

Examples of *in vivo* peak systolic velocity MIP and the cohort-averaged AA and DA flow waveforms obtained using conventional 4D flow and k-t accelerated acquisitions with the linear k-space reordering are shown in Figure 4a and 4b, respectively. Comprehensive results of all eight k-t accelerated acquisitions are shown in Supporting Figure S3, illustrating similar flow dynamics across the cardiac cycle for all nine 4D flow scans. Results of regional flow quantification are summarized in Table 3. Discrepancies between k-t accelerated and conventional 4D flow MRI ranged on average from −18 to 11% for Vmax, −15 to 3% for Qmax and −17 to 2.9% for Qnet. The best performance compared to conventional 4D flow MRI was found for the linear (Vmax: −4.5 to 6.4%, Qmax: −4.2 to 3% and Qnet: −3.2 to 1.6% errors) and out-center-out (Vmax: −3.4 to 11%, Qmax: −3.9 to −1.1% and Qnet: −5.3 to 2.9% errors) k_y-k_z sampling patterns. Notably, hemodynamic parameters obtained from k-t accelerated 4D flow MRI with both out-center-out and linear k-space samplings were similar compared to conventional 4D flow MRI (no significant differences for any index or aortic region, $p \geq 0.05$). In contrast, center-out sampling resulted in significant differences against conventional 4D flow MRI for almost all hemodynamic indices.

Finally, the results of the Bland-Altman analysis comparing hemodynamic indices for each free breathing k-t accelerated dataset against conventional 4D flow are provided in the supporting material. Mean biases and limits of agreement are summarized in Supporting Table S1, while the corresponding Bland-Altman diagrams are provided in Supporting Figures S4–6. Supporting Figure S7 further illustrates bar plots for comparison between mean biases obtained with the various k_y-k_z sampling patterns and spatial resolutions. This analysis reveals overall lowest biases compared to conventional 4D flow MRI when using the out-center-out k_y-k_z sampling pattern (mean biases [limits of agreement]: from −6.3 [−39;26] to 7.4 [−27;41] cm/s for Vmax, −12 [−73;49] to −8.9 [−120;103] ml/s for Qmax, −2.7 [−13;7.2] to 1.1 [−13;15] ml for Qnet).

Patient study

Using the results from the healthy volunteers study, we further investigated the performance of the k-t accelerated free breathing 4D flow MRI using the best spatial resolution SRes1 and the out-center-out k_y-k_z sampling pattern in 10 patients. Among them, 6 had a native tricuspid aortic valve, 2 had a bicuspid aortic valve and 3 had undergone surgery for aortic valve replacement (n=2) or aneurysm repair (n=1) in the past. Two patients had moderate to severe aortic valve stenosis, while 5 had trace to moderate aortic valve regurgitation. Sinus of Valsalva and mid-ascending aorta mean diameters were 41±5.6 and 44±13 mm, respectively. All patients had normal left ventricular ejection fraction (mean value=59±4%).

Conventional respiration-controlled and free breathing k-t accelerated 4D flow MRI scan times obtained in patients are provided in Table 5 (top row), confirming significantly reduced scan time for the k-t accelerated technique (p=0.002). Examples of magnitude images and 3D PC-MRA MIP obtained in a patient with a large thoracic aortic aneurysm (sinus of Valsalva / mid-AA diameters = 40 / 75 mm) as well as stenosis of the tricuspid aortic valve, using pre-operative conventional and k-t accelerated 4D flow MRI, are shown in Figure 5a. Grading for edge sharpness, signal and noise in the AA, arch and DA, averaged over the 10 patients are provided in Table 5 (middle row), indicating similar image quality between conventional and k-t accelerated 4D flow data. Median grading reached 3 for almost all criteria, except for DA wall edge sharpness which was reduced when using k-t accelerated 4D flow, albeit non-significantly. Finally, Figures 5b and 5c illustrate peak systolic velocity MIPs calculated for the aforementioned patient, as well as AA and DA flow rate waveforms averaged over the 10 patients, as obtained using conventional and k-t accelerated 4D flow sequences. The quantitative comparison between the two techniques in terms of hemodynamic parameters is summarized in Table 5 (bottom rows). Again, similar ranges as in the volunteer study for errors, mean biases and limits of agreement were found. Peak velocity in patients was more systematically underestimated with the k-t accelerated approach which had a lower resolution when compared to the conventional respiration-controlled 4D flow reference. Most importantly, differences in all hemodynamic parameters and all locations were non-significant.

Discussion

The purpose of this study was to achieve aortic 4D flow MRI acquisition within 2 minutes, using k-t PEAK GRAPPA, adapted spatial and temporal resolutions as well as no respiratory control. The performance of this strategy was assessed on an *in vitro* aortic coarctation model, in 10 healthy volunteers as well as 10 patients with various aortic diseases. Our main findings were that: 1) aortic 4D flow under 2 minutes is feasible but can lead to a moderate underestimation of hemodynamic indices and particularly of peak systolic velocity; 2) free breathing without controlling for respiration motion reduces image quality but flow and velocity indices for specific k-space ordering schemes (linear, out-center-out) were not significantly different from those obtained using conventional navigator-gated 4D flow; 3) the observed differences in k-space sampling patterns suggest an opportunity to mitigate some image artifacts and velocity errors by adapting k-space filling. Thus, the methods presented here are potentially useful for rapid 4D flow MRI for aortic flow quantification,

although care has to be taken when applied to regions where complex flow dynamics and high velocities are expected, such as coarctation or valvular dysfunction. The encouraging results still need more investigation to identify the optimal combination between acceleration, resolution, k-space sampling pattern and respiration control.

The *in vitro* experiments using a patient-specific 3D printed aortic coarctation model showed that the use of k-t acceleration and decreased spatial and temporal resolutions predictably lead to a systematic underestimation of peak velocity and flow indices, when compared to conventional 4D flow MRI. However, differences were small (absolute differences below 11% for flow parameters and <13% for AA and arch peak velocity), except for peak velocity in the descending aorta at the location of the coarctation where complex flow requires high spatial and temporal resolutions to capture abrupt local hemodynamic alterations accurately. Data from both healthy and diseased populations allowed to further study the effect of discarding respiratory control. Although image quality was systematically better when using the conventional navigator-gated 4D flow, differences were not significant when considering the k-t accelerated datasets acquired with the lowest resolution (SRes2). We hypothesize that this might be due to the shorter acquisition, i.e. overall less respiratory cycles, or to the fact that voxel size was closer to the order of magnitude of respiratory motion in the images. When comparing the four k_y-k_z sampling patterns in the healthy volunteers, we found that differences between conventional and k-t accelerated 4D flow were significant for most of the aortic hemodynamic indices when using the center-out strategy, while hemodynamic metrics were in good agreement when considering the linear and out-center-out patterns. In addition, the lowest mean biases were obtained with the out-center-out pattern (Figure S4). Our hypothesis when implementing this sampling pattern was that prioritizing the acquisition of the k-space center once a stable physiological state and respiratory pattern of the patient was reached would favor image contrast. Indeed, it seems on our small group that this strategy provided superior results than when starting directly the acquisition by filling the k-space center (‘center-out’ filling pattern), while still filling the k-space corners at the beginning of the acquisition in order to keep the same short scan time. It might be due to the fact that a transient phase is needed to ensure patient physiology and respiration stability.

Other groups have reported on the combination of imaging acceleration and 4D flow MRI, including advanced multidimensional parallel imaging such as k-t schemes (7–9,19–21), or sampling methods such as compressed sensing (5) and non-Cartesian radial acquisition (6). As an example, radial imaging with 3D PC vastly undersampled isotropic projection (VIPR) allows highly accelerated acquisition while maintaining good image quality as demonstrated in the brain (6). In addition to k-t-GRAPPA (9), whose feasibility at 7T and ability to reduce aortic 4D flow scan time while maintaining accurate flow quantification were recently demonstrated (20), several other multidimensional parallel imaging methods were previously proposed in the literature to address long acquisition time. Two of these methods are the k-t SENSE and k-t BLAST acceleration techniques, which were first validated with 2D PC MRI by Baltes et al. (8). In this study, the *in vivo* application of k-t SENSE and k-t BLAST in 6 healthy volunteers resulted in good image quality, with an expected temporal blurring at high (8-fold) accelerations, although no quantitative scoring was performed (8). When comparing AA stroke volume against measurements obtained with a non-accelerated PC sequence, the authors reported k-t accelerated / non-accelerated ratios of 106±18% and

112±15% (reported as mean±2xstandard deviation) for k-t SENSE with acceleration factors R=5 and 8, respectively. These values are in agreement with findings from our volunteer study (k-t accelerated / conventional 4D flow ratio for SRes1: 102±24% and 102±28%; SRes2: 100±34% and 103±24%, with linear and out-center-out k-space sampling patterns, respectively). Of note, our larger standard deviations might be due to the fact that Baltes et al. used the same temporal and spatial resolutions between accelerated and non-accelerated sequences.

A more recent study compared the performance of non-respiratory controlled k-t BLAST 4D flow against gated SENSE 4D flow and 2D SENSE PC MRI (21). In line with our findings, the authors reported significantly reduced 4D flow scan times (5-fold) between k-t BLAST (averaged in 15 healthy volunteers and 8 patients with surgically repaired aortic coarctation: 5.5 minutes) and gated SENSE (21). However, they found that the quality of magnitude images was significantly better when using k-t accelerated acquisitions. This discrepancy with our results might be due to differences in the employed techniques (Zaman et al. (21): k-t BLAST vs. SENSE; our study: PEAK GRAPPA vs. GRAPPA). However, the mean biases reported in their study for comparison between aortic hemodynamic indices were in the same range as ours: from 3.2 to 11.6 cm/s for Vmax (our study: SRes1: −7.9 to 7.4 cm/s; SRes2: −6.3 to 1.3 cm/s, with the out-center-out k-space sampling pattern), 5.4 to 11.2 ml/s for Qmax (our study: SRes1: −11 to −3.8 and SRes2: −12 to −10 ml/s), and −0.1 to 0.1 ml for Qnet (our study: SRes1: −2.3 to 5.8 and SRes2: −2.7 to 1.1 ml).

Another multidimensional parallel imaging method is the compartment-based k-t principal component analysis (PCA), which was first applied to 4D flow MRI by Giese et al. (19) and was shown to reduce temporal blurring with a net acceleration factor R=8 when compared to k-t SENSE, while leading to accurate aortic stroke volume quantification. In their *in vivo* study including 6 healthy volunteers, they reported mean biases close to ours for comparison of fully sampled datasets with k-t SENSE, regular k-t PCA and compartment k-t PCA, respectively: −1.7±6.1, 0.4±5.0 and −0.1±4.9 ml (our volunteer study: SRes1: 0.1±8.5 and −2.3±3.1 ml; SRes2: 1.1±7.0 and −2.7±5.0 ml, for net volume in the AA and DA, respectively, with the out-center-out k-space sampling pattern).

Other studies combined several of these MRI methods, such as parallel imaging and compressed sensing. It was indeed successfully applied to 4D flow MRI in pediatric populations (22–24). However no comparison with conventional 4D flow was reported, but rather qualitative assessment of valvular insufficiency, intra- and extra-cardiac shunts as well as postsurgical leaks, interobserver agreement (which was found to be high) and comparison against echocardiography (resulting in a good agreement) (23), consistency of venous and arterial flow conservation (24), or comparison of ventricular volumes against SSFP and of flow rates against 2D PC (22).

Another combination between spiral sampling and dynamic compressed sensing allowed for the acquisition of abdominal 4D flow MRI in a breath-hold (over 24 heart beats) (25). This study investigated its application in 3 healthy volunteers and 7 patients with liver disease. Although no significant differences in arterial and venous wall sharpness were obtained between gated Cartesian and the proposed breath-held spiral 4D flow, significantly more

background artifacts were found when using the latter (grading 2.0 vs. 2.9) (25). In addition, the authors reported that spiral flow measurements were significantly lower and that peak velocity was similar to the ones provided by the gated Cartesian 4D flow. They further observed significantly lower vessel area with spiral 4D flow, which might be due to the breath-hold and also to the fact that abdominal vessels are smaller than the aorta and thus more sensitive to resolution and partial volume effects.

In addition to advanced acquisition schemes, several cardiovascular 4D flow MRI studies have investigated the effect of respiratory motion control (4,26–29). Most studies used navigator gating as the reference method for comparison, and reported overall good agreement between gated and non-gated datasets, in terms of AA stroke volume (28), global aortic velocity vector fields (4), or intracardiac flow indices such as stroke volume, kinetic energy and vortex ring volume (27). In the latter study, however, the authors found a better correlation compared to 2D PC MRI when using 4D flow gated acquisitions (27). This may be due to the fact that intra-cardiac measurements could be more sensitive to breathing motion than for the aorta. More advanced methods for respiratory motion correction were proposed, such as self-gating methods which can be applied either retrospectively, prospectively (30–32) or in real time (29). Aortic stroke volume was found to be lower, and agreement against 2D PC MRI measurements was found to be reduced, for non-gated acquisitions compared to real-time self-gated 4D flow (29). This discrepancy with our results can be explained by the different methods used for respiratory control. In addition, a limitation of this study is that the authors considered the non-gated measurements while averaging 2 scans to match acquisition time (12 minutes) of the self-gated scan, thereby averaging measurements over more cardiac cycles and not taking full advantage of a non-gated scan, i.e. reduced scan time. Finally, Andersson et al. reported the comparison between navigator-gated and breath-held non-gated cardiac 2D PC MRI (26); however, differences in aortic hemodynamics were previously shown to be related to the difference in respiratory state between free breathing and breath-holding (33). All these findings indicate that, in some cases, respiratory control might be omitted for 4D flow acquisitions. Another alternative is the combination of compressed sensing and motion compensation, as recently developed in a 4D flow MRI study for pediatric congenital heart disease applications (34), resulting in good interobserver agreement and consistency between aortic and pulmonary flow. In the context of our objectives, all these acceleration and respiratory control methods are of interest and should be explored in future studies to compromise between short scan time and breathing motion correction.

A main limitation of our work is the low number of subjects. Although the results reported here are encouraging, care should be taken regarding statistical interpretation. In addition, a test-retest reproducibility study is lacking. Another drawback is that only one k-t accelerated 4D flow MRI strategy was evaluated in the patients, instead of 8 in the healthy volunteers. However, even though the whole scan session required no breath-holding, it was difficult to add the 7 other sequences on the clinical protocol. In addition, we did not simulate respiration in the phantom scans; rather, these were used to understand the impact of acceleration and decreased spatio-temporal resolution. The volunteer and patient studies were used to evaluate respiratory control effects. Furthermore, it would be interesting to compare *in vivo* in a future work the different existing respiration motion correction

methods, as was recently performed using numerical simulations (35). Finally, technical limitations include the anisotropic voxel size, and long reconstruction times when using the PEAK GRAPPA method, which was up to 10 minutes for the SRes1 datasets. These should be addressed in future efforts.

In conclusion, we showed that aortic 4D flow acquisition under 2 minutes was feasible and easy to use, with no navigator placement and set-up required before the actual acquisition. The results presented in this preliminary study on an *in vitro* phantom as well as in healthy volunteers and patients with aortic disease, in terms of flow index quantification, are promising for performing hemodynamic measurements in a short period of time to complement standard of care assessment of cardiovascular flow. However, further investigation is needed to improve image quality as well as accurate quantification of complex flow, and to define the best compromise between imaging acceleration, resolution and k-space sampling patterns to mitigate respiratory motion.

Supplementary Material

Refer to Web version on PubMed Central for supplementary material.

Acknowledgments

Grant support

This work was supported by the National Institutes of Health grants R01HL115828 and K25HL119608 as well as the American Heart Association Midwest Affiliate grant 16POST27250158.

References

1. Pelc NJ, Herfkens RJ, Shimakawa A, Enzmann DR. Phase contrast cine magnetic resonance imaging. Magnetic resonance quarterly. 1991; 7(4):229–254. [PubMed: 1790111]
2. Dyverfeldt P, Bissell M, Barker AJ, Bolger AF, Carlhall CJ, Ebbers T, Francios CJ, Frydrychowicz A, Geiger J, Giese D, Hope MD, Kilner PJ, Kozerke S, Myerson S, Neubauer S, Wieben O, Markl M. 4D flow cardiovascular magnetic resonance consensus statement. Journal of cardiovascular magnetic resonance : official journal of the Society for Cardiovascular Magnetic Resonance. 2015; 17:72. [PubMed: 26257141]
3. Wang Y, Riederer SJ, Ehman RL. Respiratory motion of the heart: kinematics and the implications for the spatial resolution in coronary imaging. Magnetic resonance in medicine. 1995; 33(5):713–719. [PubMed: 7596276]
4. van Ooij P, Semaan E, Schnell S, Giri S, Stankovic Z, Carr J, Barker AJ, Markl M. Improved respiratory navigator gating for thoracic 4D flow MRI. Magnetic resonance imaging. 2015; 33(8): 992–999. [PubMed: 25940391]
5. Lustig M, Donoho D, Pauly JM. Sparse MRI: The application of compressed sensing for rapid MR imaging. Magnetic resonance in medicine. 2007; 58(6):1182–1195. [PubMed: 17969013]
6. Johnson KM, Lum DP, Turski PA, Block WF, Mistretta CA, Wieben O. Improved 3D phase contrast MRI with off-resonance corrected dual echo VIPR. Magnetic resonance in medicine. 2008; 60(6): 1329–1336. [PubMed: 19025882]
7. Griswold MA, Jakob PM, Heidemann RM, Nittka M, Jellus V, Wang J, Kiefer B, Haase A. Generalized autocalibrating partially parallel acquisitions (GRAPPA). Magnetic resonance in medicine. 2002; 47(6):1202–1210. [PubMed: 12111967]
8. Baltes C, Kozerke S, Hansen MS, Pruessmann KP, Tsao J, Boesiger P. Accelerating cine phase-contrast flow measurements using k-t BLAST and k-t SENSE. Magnetic resonance in medicine. 2005; 54(6):1430–1438. [PubMed: 16276492]

9. Jung B, Stalder AF, Bauer S, Markl M. On the undersampling strategies to accelerate time-resolved 3D imaging using k-t-GRAPPA. Magnetic resonance in medicine. 2011; 66(4):966–975. [PubMed: 21437975]
10. Markl M, Harloff A, Bley TA, Zaitsev M, Jung B, Weigang E, Langer M, Hennig J, Frydrychowicz A. Time-resolved 3D MR velocity mapping at 3T: improved navigator-gated assessment of vascular anatomy and blood flow. Journal of magnetic resonance imaging : JMRI. 2007; 25(4): 824–831. [PubMed: 17345635]
11. Jung B, Ullmann P, Honal M, Bauer S, Hennig J, Markl M. Parallel MRI with extended and averaged GRAPPA kernels (PEAK-GRAPPA): optimized spatiotemporal dynamic imaging. Journal of magnetic resonance imaging : JMRI. 2008; 28(5):1226–1232. [PubMed: 18972331]
12. Schnell S, Markl M, Entezari P, Mahadewia RJ, Semaan E, Stankovic Z, Collins J, Carr J, Jung B. k-t GRAPPA accelerated four-dimensional flow MRI in the aorta: effect on scan time, image quality, and quantification of flow and wall shear stress. Magnetic resonance in medicine. 2014; 72(2):522–533. [PubMed: 24006309]
13. Allen BD, Barker AJ, Carr JC, Silverberg RA, Markl M. Time-resolved three-dimensional phase contrast MRI evaluation of bicuspid aortic valve and coarctation of the aorta. European heart journal cardiovascular Imaging. 2013; 14(4):399. [PubMed: 23111692]
14. Lorenz R, Benk C, Bock J, Stalder AF, Korvink JG, Hennig J, Markl M. Closed circuit MR compatible pulsatile pump system using a ventricular assist device and pressure control unit. Magnetic resonance in medicine. 2012; 67(1):258–268. [PubMed: 21630351]
15. Benk C, Mauch A, Beyersdorf F, Klemm R, Russe M, Blanke P, Korvink JG, Markl M, Jung B. Effect of cannula position in the thoracic aorta with continuous left ventricular support: four-dimensional flow-sensitive magnetic resonance imaging in an in vitro model. European journal of cardio-thoracic surgery : official journal of the European Association for Cardio-thoracic Surgery. 2013; 44(3):551–558. [PubMed: 23449865]
16. Schnell S, Entezari P, Mahadewia RJ, Malaisrie SC, McCarthy PM, Collins JD, Carr J, Markl M. Improved Semiautomated 4D Flow MRI Analysis in the Aorta in Patients With Congenital Aortic Valve Anomalies Versus Tricuspid Aortic Valves. Journal of computer assisted tomography. 2016; 40(1):102–108. [PubMed: 26466113]
17. Rose MJ, Jarvis K, Chowdhary V, Barker AJ, Allen BD, Robinson JD, Markl M, Rigsby CK, Schnell S. Efficient method for volumetric assessment of peak blood flow velocity using 4D flow MRI. Journal of magnetic resonance imaging : JMRI. 2016
18. Stalder AF, Russe MF, Frydrychowicz A, Bock J, Hennig J, Markl M. Quantitative 2D and 3D phase contrast MRI: optimized analysis of blood flow and vessel wall parameters. Magnetic resonance in medicine. 2008; 60(5):1218–1231. [PubMed: 18956416]
19. Giese D, Schaeffter T, Kozerke S. Highly undersampled phase-contrast flow measurements using compartment-based k-t principal component analysis. Magnetic resonance in medicine. 2013; 69(2):434–443. [PubMed: 22528878]
20. Schmitter S, Schnell S, Ugurbil K, Markl M, Van de Moortele PF. Towards high-resolution 4D flow MRI in the human aorta using kt-GRAPPA and B1+ shimming at 7T. Journal of magnetic resonance imaging : JMRI. 2016; 44(2):486–499. [PubMed: 26841070]
21. Zaman A, Motwani M, Oliver JJ, Crelier G, Dobson LE, Higgins DM, Plein S, Greenwood JP. 3. 0T, time-resolved, 3D flow-sensitive MR in the thoracic aorta: Impact of k-t BLAST acceleration using 8-versus 32-channel coil arrays. Journal of magnetic resonance imaging : JMRI. 2015; 42(2):495–504. [PubMed: 25447784]
22. Hsiao A, Lustig M, Alley MT, Murphy M, Chan FP, Herfkens RJ, Vasanawala SS. Rapid pediatric cardiac assessment of flow and ventricular volume with compressed sensing parallel imaging volumetric cine phase-contrast MRI. AJR American journal of roentgenology. 2012; 198(3):W250–259. [PubMed: 22358022]
23. Hsiao A, Lustig M, Alley MT, Murphy MJ, Vasanawala SS. Evaluation of valvular insufficiency and shunts with parallel-imaging compressed-sensing 4D phase-contrast MR imaging with stereoscopic 3D velocity-fusion volume-rendered visualization. Radiology. 2012; 265(1):87–95. [PubMed: 22923717]
24. Tariq U, Hsiao A, Alley M, Zhang T, Lustig M, Vasanawala SS. Venous and arterial flow quantification are equally accurate and precise with parallel imaging compressed sensing 4D phase

contrast MRI. Journal of magnetic resonance imaging : JMRI. 2013; 37(6):1419–1426. [PubMed: 23172846]

25. Dyvorne H, Knight-Greenfield A, Jajamovich G, Besa C, Cui Y, Stalder A, Markl M, Taouli B. Abdominal 4D flow MR imaging in a breath hold: combination of spiral sampling and dynamic compressed sensing for highly accelerated acquisition. Radiology. 2015; 275(1):245–254. [PubMed: 25325326]
26. Andersson C, Kihlberg J, Ebbers T, Lindstrom L, Carlhall CJ, Engvall JE. Phase-contrast MRI volume flow--a comparison of breath held and navigator based acquisitions. BMC medical imaging. 2016; 16:26. [PubMed: 27021353]
27. Kanski M, Toger J, Steding-Ehrenborg K, Xanthis C, Bloch KM, Heiberg E, Carlsson M, Arheden H. Whole-heart four-dimensional flow can be acquired with preserved quality without respiratory gating, facilitating clinical use: a head-to-head comparison. BMC medical imaging. 2015; 15:20. [PubMed: 26080805]
28. Nordmeyer S, Riesenkampff E, Crelier G, Khasheei A, Schnackenburg B, Berger F, Kuehne T. Flow-sensitive four-dimensional cine magnetic resonance imaging for offline blood flow quantification in multiple vessels: a validation study. Journal of magnetic resonance imaging : JMRI. 2010; 32(3):677–683. [PubMed: 20815066]
29. Uribe S, Beerbaum P, Sorensen TS, Rasmusson A, Razavi R, Schaeffter T. Four-dimensional (4D) flow of the whole heart and great vessels using real-time respiratory self-gating. Magnetic resonance in medicine. 2009; 62(4):984–992. [PubMed: 19672940]
30. Brau AC, Brittain JH. Generalized self-navigated motion detection technique: Preliminary investigation in abdominal imaging. Magnetic resonance in medicine. 2006; 55(2):263–270. [PubMed: 16408272]
31. Buehrer M, Curcic J, Boesiger P, Kozerke S. Prospective self-gating for simultaneous compensation of cardiac and respiratory motion. Magnetic resonance in medicine. 2008; 60(3): 683–690. [PubMed: 18727084]
32. Larson AC, Kellman P, Arai A, Hirsch GA, McVeigh E, Li D, Simonetti OP. Preliminary investigation of respiratory self-gating for free-breathing segmented cine MRI. Magnetic resonance in medicine. 2005; 53(1):159–168. [PubMed: 15690515]
33. Bollache E, van Ooij P, Powell A, Carr J, Markl M, Barker AJ. Comparison of 4D flow and 2D velocity-encoded phase contrast MRI sequences for the evaluation of aortic hemodynamics. The international journal of cardiovascular imaging. 2016
34. Cheng JY, Hanneman K, Zhang T, Alley MT, Lai P, Tamir JI, Uecker M, Pauly JM, Lustig M, Vasanawala SS. Comprehensive motion-compensated highly accelerated 4D flow MRI with ferumoxytol enhancement for pediatric congenital heart disease. Journal of magnetic resonance imaging : JMRI. 2016; 43(6):1355–1368. [PubMed: 26646061]
35. Dyverfeldt P, Ebbers T. Comparison of respiratory motion suppression techniques for 4D flow MRI. Magnetic resonance in medicine. 2017

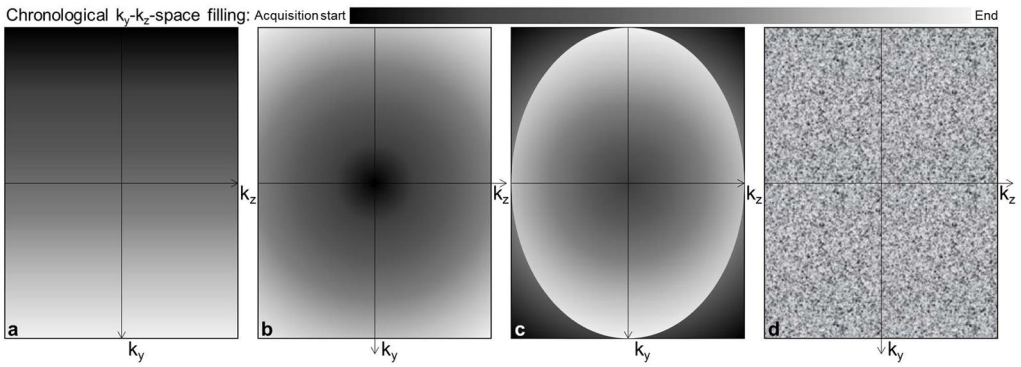

Figure 1.

Illustration of the four tested k_y-k_z-space Cartesian sampling strategies: a) conventional linear line-by-line k-space filling from left to right; b) closest to the furthest from the center filling (‘center-out’); c) furthest to the closest from the center during the first 10 cardiac cycles then center-out filling (‘out-center-out’); d) random filling.

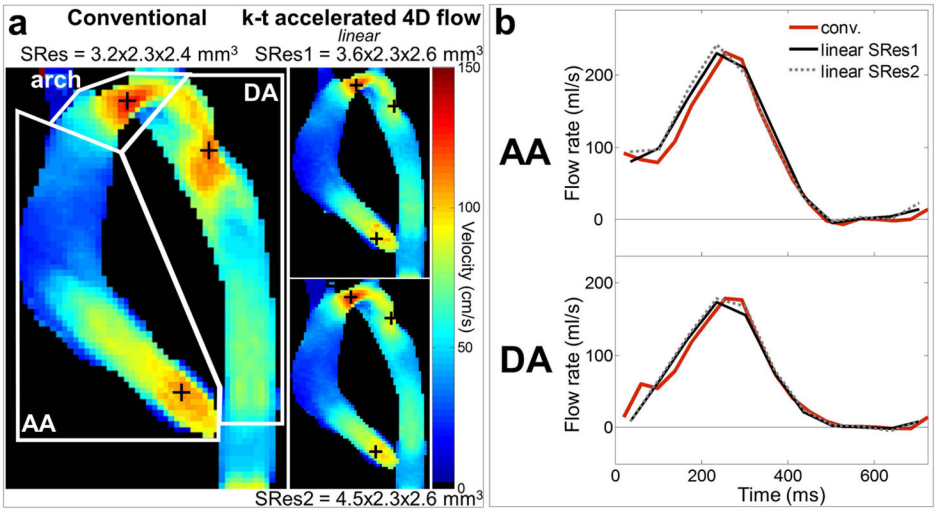

Figure 2.

In vitro 4D flow MRI experiments: a) peak systolic velocity maximal intensity projections (MIP) in sagittal orientation as obtained using conventional 4D flow (left) and k-t accelerated 4D flow with the linear k-space reordering and spatial resolutions of SRes1 = 3.6×2.3×2.6 mm^3 (top row) and SRes2 = 4.5×2.3×2.6 mm^3 (bottom row). White boxes on the conventional images define ascending (AA) and descending (DA) aorta as well as aortic arch regions. Location of AA, arch and DA peak velocities is indicated by black '+'. b) AA (top row) and DA (bottom row) flow rate waveforms throughout the cardiac cycle, as obtained using conventional 4D flow (in red) and the k-t accelerated 4D flow with linear k-space reordering and different spatial resolutions (see legend).

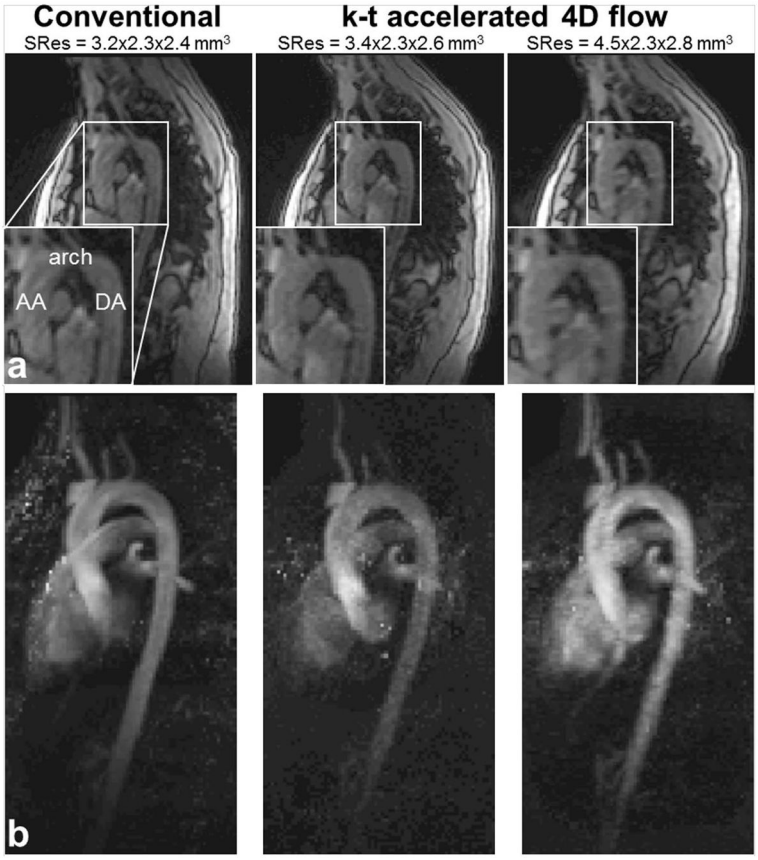

Figure 3.

Example of 4D flow data acquired in one volunteer: a) systolic magnitude images, with an emphasis on the proximal aorta (bottom left corners), and b) 3D PC-MRA sagittal maximal intensity projections (MIP) obtained using conventional respiration-controlled 4D flow (left) as well as k-t accelerated sequences with no respiration control and linear k_y-k_z-space sampling, with two different spatial resolutions (right columns).

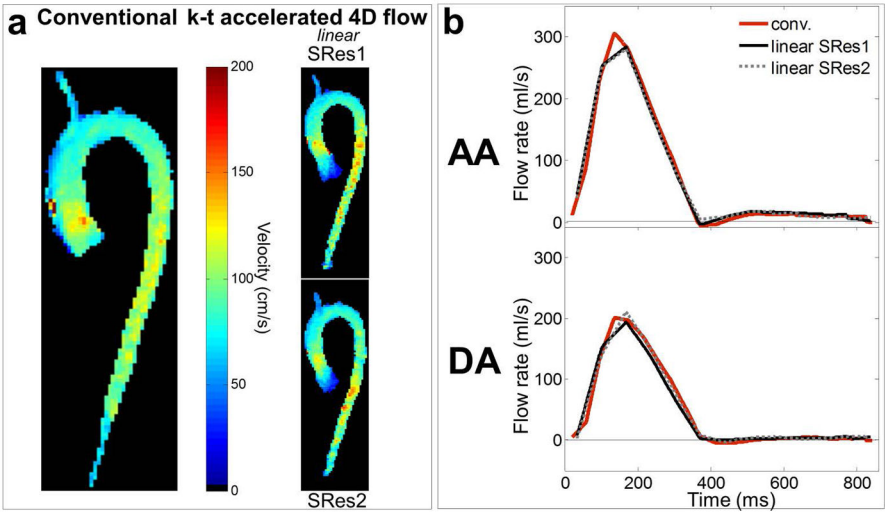

Figure 4.

In vivo 4D flow MRI volunteer studies: a) peak systolic velocity maximal intensity projections (MIP) in sagittal orientation as obtained using conventional 4D flow (left) and k-t accelerated 4D flow with the linear k-space reordering and different spatial resolutions. MIPs were eroded by one pixel to suppress border noise. b) AA (top row) and DA (bottom row) flow rate waveforms throughout the cardiac cycle averaged over the 10 volunteers, as obtained using conventional respiration-controlled 4D flow (in red) and the non-controlled k-t accelerated 4D flow with linear k-space reordering and different spatial resolutions (see legend).

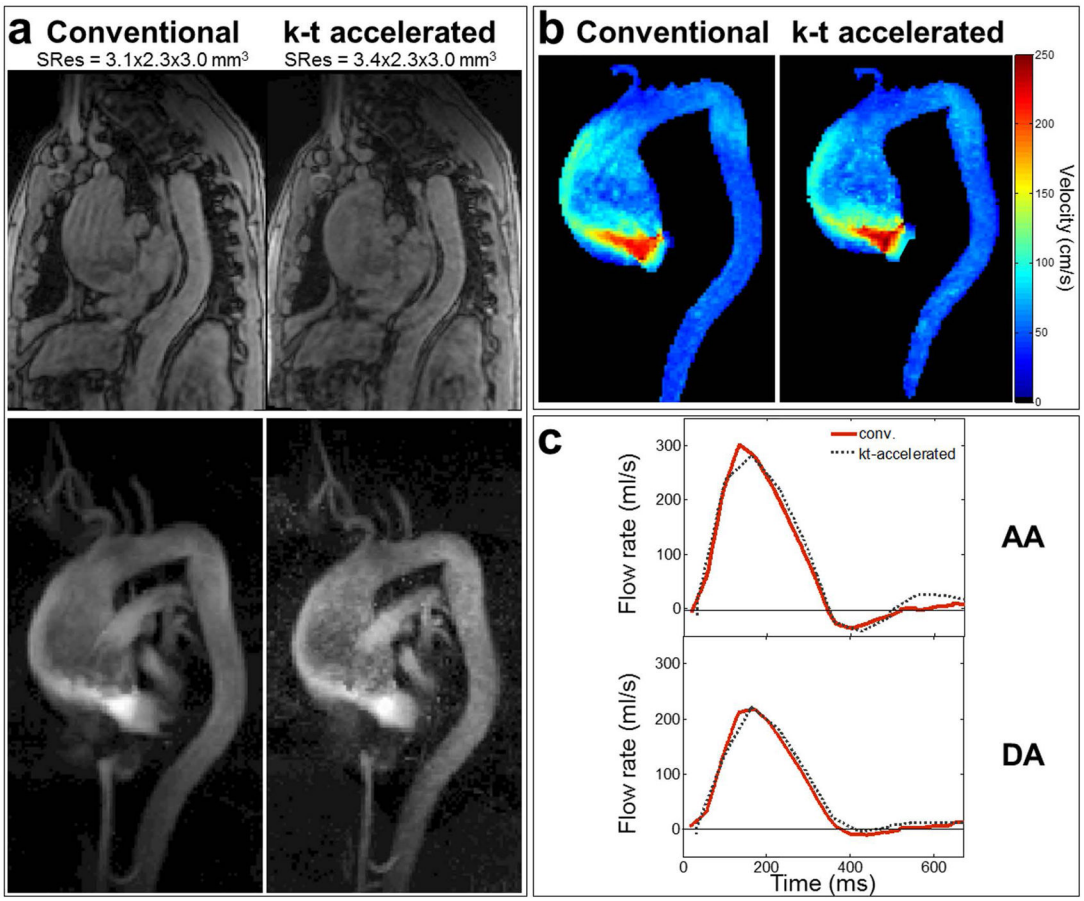

Figure 5.

Patient studies: a) example of systolic magnitude images (top) and 3D PC-MRA sagittal MIP (bottom) obtained using conventional respiration-controlled 4D flow (left) as well as k-t accelerated 4D flow with no respiration control and out-center-out k_y-k_z-space sampling (right), acquired in a patient with thoracic aortic aneurysm and moderate to severe aortic valve stenosis. b) peak systolic velocity MIP as obtained using conventional (left) and k-t accelerated (right) 4D flow in the same patient. c) AA (top) and DA (bottom) flow rate waveforms throughout the cardiac cycle averaged over the 10 patients, as obtained using conventional (in red) and k-t accelerated (grey) 4D flow.

Table 1

4D flow MRI acquisition parameters: conventional respiration-controlled 4D flow MRI (left column) and k-t accelerated 4D flow MRI with no respiration control (right columns). For the latter, data were acquired using two different spatial resolutions SRes1 and SRes2. Differences between *in vitro* aorta flow phantom and *in vivo* volunteer studies are highlighted in grey.

	Conventional	**k-t accelerated**	
	Respiration controlled	*No respiration control*	
		SRes1	**SRes2**
TR (ms)	4.9	4.2	
TE (ms)	2.5	2.3	
Flip angle (°)	*in vivo*:7 *in vitro*: 15	*in vivo*:7 *in vitro*: 15	
Acq. matrix	*in vivo*: 160x84	*in vivo*: 160x80	*in vivo*: 160x60
	in vitro: 160x112	*in vitro*: 160x100	*in vitro*: 160x80
FOV (mm^2)	*in vivo*: 360-400x270-300	*in vivo*: 360x270	
	in vitro: 360x360	*in vitro*: 360x360	
SRes (mm^3)	*in vivo*: 3.2-3.6x2.3-2.5x2.4-2.7	*in vivo*: 3.4x2.3x2.6-3.3	*in vivo*: 4.5x2.3x2.6-3.8
	in vitro: 3.2x2.3x2.4	*in vitro*: 3.6x2.3x2.6	*in vitro*: 4.5x2.3x2.6
N_{Seg}	2	4	
TRes N_{Seg}xTR (ms)	39.2	67.2	
Slices (n)	*in vivo*: 27±2 *in vitro*: 32	*in vivo*: 24 *in vitro*: 30	*in vivo*: 20 *in vitro*: 30
Venc (cm/s)	150	150	
Parallel imaging	GRAPPA (y) R=2	PEAK GRAPPA (y-z-t) R=5	

SRes: spatial resolution; TR: repetition time; TE: echo time; FOV: field of view; N_{seg}: number of k-space segments per cardiac time frame; TRes: temporal resolution; Venc: encoding sensitivity; R: acceleration factor.

Table 2

Comparison of hemodynamic parameters between *in vitro* k-t accelerated and conventional 4D flow MRI: systolic peak velocity (Vmax) in the ascending (AA) and descending (DA) aorta as well the aortic arch, AA and DA flow peak (Qmax) and net volume (Qnet). Conventional 4D flow parameters are reported in the left column. k-t accelerated 4D flow parameters were obtained using different k-space reorderings (linear, 'center-out', 'out-center-out', random) and spatial resolutions of 3.6×2.3×2.6 mm^3 and 4.5×2.3×2.6 mm^3. Relative differences (in %) between k-t accelerated and conventional measurements are provided in grey.

	Conventional	**k-t accelerated**							
SRes	**3.2×2.3×2.4 mm^3**	**3.6×2.3×2.6 mm^3**				**4.5×2.3×2.6 mm^3**			
		linear	***center-out***	***out-center-out***	***random***	***linear***	***center-out***	***out-center-out***	***random***
Peak velocity Vmax (cm/s)									
AA	1.08	0.94	0.99	0.96	0.97	0.94	0.98	0.95	0.96
arch	1.30	1.23	1.27	1.29	1.26	1.27	1.28	1.26	1.25
DA (coarct.)	1.16	0.90	0.94	0.95	0.91	0.96	0.93	0.93	0.95
Flow peak Qmax (ml/s)									
AA	231	229	233	230	222	242	241	237	241
DA (coarct.)	178	173	174	178	172	179	185	179	175
Net volume Qnet (ml)									
AA	56.9	60.6	60.7	62.5	59.7	61.0	62.6	63.3	62.1
DA (coarct.)	42.6	41.6	41.5	42.5	41.8	43.7	44.6	42.8	41.8

Magn Reson Med. Author manuscript; available in PMC 2019 January 01.

Table 3

Comparison of scan times and hemodynamic parameters between *in vivo* volunteer k-t accelerated and conventional 4D flow MRI: peak velocity (Vmax) in the ascending (AA) and descending (DA) aorta as well the aortic arch, AA and DA flow peak (Qmax) and net volume (Qnet). Conventional respiration-controlled 4D flow results are provided in the left column. Non-controlled k-t accelerated 4D flow was performed with 4 different k-space reorderings (linear, 'center-out', 'out-center-out', random) and 2 spatial resolutions. Relative differences (in %) between k-t accelerated and conventional measurements are provided in grey.

Conventional		**k-t accelerated**							
		SRes1				**SRes2**			
		linear	***center-out***	***out-center-out***	***random***	***linear***	***center-out***	***out-center-out***	***random***
Scan time (min)									
	11:56±1:30	**2:03±0:16** *	**1:58±0:16** *	**1:56±0:15** *	**1:57±0:15** *	**1:25±0:11** *	**1:26±0:11** *	**1:25±0:11** *	**1:26±0:11** *
Peak velocity Vmax (cm/s)									
AA	164±32	161±31	**134±23** *	162±25	159±22	156±26	**141±22** *	158±32	**150±27** *
arch	82±17	86±18	78±15	89±18	83±14	82±16	**73±13** *	83±14	79±13
DA	97±22	100±19	**83±12** *	99±21	95±20	98±20	**80±13** *	93±14	93±16
Flow peak Qmax (ml/s)									
AA	309±88	298±70	**267±62** *	300±81	290±72	294±91	**268±66** *	299±77	286±64
DA	211±56	200±46	**176±41** *	200±46	**188±42** *	214±56	**181±42** *	199±48	190±44
Net volume Qnet (ml)									
AA	59±13	59±11	**53±10** *	59±11	59±13	58±11	56±13	60±11	60±12

	Conventional	k-t accelerated							
		SRes1				SRes2			
		linear	*center-out*	*out-center-out*	*random*	*linear*	*center-out*	*out-center-out*	*random*
DA	40±9.1	38±7.5	**33±7.8** *	38±7.3	**35±7.1** *	40±9.4	**34±6.5** *	37±7.8	**36±8.0** *

* indicates p<0.05 vs. conventional respiration-controlled measurement

Table 4

Results of image quality grading (as median (interquartile range) over the 10 volunteers), obtained with conventional respiration-controlled 4D flow MRI as well as k-t accelerated datasets using 4 different k-space sampling strategies and 2 spatial resolutions.

	Conventional	**k-t accelerated**							
		SRes1				**SRes2**			
		linear	***center-out***	***out-center-out***	***random***	***linear***	***center-out***	***out-center-out***	***random***
Edge sharpness									
AA	3.0 (3.0–3.0)	3.0 (2.3–3.0)	2.5 (2.0–3.0)	3.0 (2.0–3.0)	3.0 (2.0–3.0)	3.0 (3.0–3.0)	3.0 (2.3–3.0)	3.0 (3.0–3.0)	3.0 (3.0–3.0)
arch	3.0 (3.0–3.0)	2.5 (2.0–3.0)	2.5 (2.0–3.0)	2.5 (2.0–3.0)	2.5 (2.0–3.0)	3.0 (2.3–3.0)	3.0 (2.0–3.0)	3.0 (2.3–3.0)	3.0 (2.0–3.0)
DA	3.0 (3.0–3.0)	**2.0 (1.0–2.8)** *	2.5 (2.0–3.0)	**2.0 (2.0–2.8)** *	**2.0 (1.3–3.0)** *	2.5 (2.0–3.0)	3.0 (2.0–3.0)	3.0 (2.0–3.0)	3.0 (2.0–3.0)
Signal									
AA	3.0 (3.0–3.0)	3.0 (2.0–3.0)	3.0 (3.0–3.0)	3.0 (2.0–3.0)	3.0 (2.3–3.0)	3.0 (3.0–3.0)	3.0 (3.0–3.0)	3.0 (3.0–3.0)	3.0 (3.0–3.0)
arch	3.0 (3.0–3.0)	2.5 (2.0–3.0)	3.0 (2.3–3.0)	**2.0 (2.0–3.0)** *	2.5 (2.0–3.0)	3.0 (2.0–3.0)	3.0 (2.3–3.0)	3.0 (2.0–3.0)	3.0 (2.3–3.0)
DA	3.0 (2.0–3.0)	**1.5 (1.0–2.0)** *	2.5 (1.3–3.0)	**2.0 (1.3–2.0)** *	2.0 (1.3–2.8)	2.5 (1.3–3.0)	3.0 (2.3–3.0)	2.0 (2.0–3.0)	2.5 (2.0–3.0)
Noise									
AA	3.0 (3.0–3.0)	**2.0 (2.0–2.8)** *	3.0 (2.0–3.0)	**2.0 (2.0–3.0)** *	2.5 (2.0–3.0)	2.5 (2.0–3.0)	3.0 (2.3–3.0)	3.0 (2.0–3.0)	2.5 (2.0–3.0)
arch	3.0 (3.0–3.0)	**2.0 (2.0–2.3)** *	3.0 (2.0–3.0)	2.0 (2.0–3.0)	2.5 (2.0–3.0)	2.0 (2.0–3.0)	3.0 (2.3–3.0)	3.0 (2.0–3.0)	2.0 (2.0–3.0)
DA	2.0 (2.0–3.0)	2.0 (2.0–2.8)	2.0 (2.0–3.0)	2.0 (2.0–2.0)	2.0 (2.0–2.0)	2.0 (2.0–2.0)	3.0 (2.0–3.0)	2.0 (2.0–2.0)	2.0 (2.0–2.3)

* indicates $p<0.05$ vs. conventional grading

Table 5

Comparison in patients of scan times (top row), image quality grading (middle) and hemodynamic parameters (bottom rows) between k-t accelerated (right) and conventional respiration-controlled (left) 4D flow MRI. Non-controlled k-t accelerated 4D flow was performed with the 'out-center-out' k-space reordering and the SRes1 spatial resolution. Relative differences (in %) as well as mean biases [limits of agreement] between k-t accelerated and conventional measurements are provided for each hemodynamic index in grey: peak velocity (Vmax) in the ascending (AA) and descending (DA) aorta as well the aortic arch, AA and DA flow peak (Qmax) and net volume (Qnet).

	Conventional	**k-t accelerated**
	Respiration controlled	***No respiration control*** **SRes1**
		out-center-out
Scan time (min)		
	12:47±2:53	**2:05±0:44** *
Image quality grading: edge sharpness		
AA	3.0 (2.3–3.0)	3.0 (2.0–3.0)
arch	3.0 (3.0–3.0)	3.0 (2.0–3.0)
DA	3.0 (2.3–3.0)	2.0 (2.0–2.8)
Signal		
AA	3.0 (3.0–3.0)	3.0 (3.0–3.0)
arch	3.0 (3.0–3.0)	3.0 (3.0–3.0)
DA	3.0 (3.0–3.0)	3.0 (3.0–3.0)
Noise		
AA	3.0 (3.0–3.0)	3.0 (2.3–3.0)
arch	3.0 (3.0–3.0)	3.0 (3.0–3.0)
DA	3.0 (3.0–3.0)	3.0 (3.0–3.0)
Hemodynamic parameters: peak velocity Vmax (cm/s)		
AA	192±55	184±54
arch	112±55	106±56
DA	95±22	89±17
Flow peak Qmax (ml/s)		
AA	308±92	296±89

	Conventional	k-t accelerated
	Respiration controlled	***No respiration control*** **SRes1**
		out-center-out
DA	234±53	223±40
Net volume Qnet (ml)		
AA	50±16	52±19
DA	41±9.1	44±8.8

* indicates $p<0.05$ vs. conventional respiration-controlled measurement